Computers and Concrete, *Vol. 16, No. 4 (2015) 605-623*
DOI: http://dx.doi.org/10.12989/cac.2015.16.4.605

Influence of the inclined edge notches on the shear-fracture behavior in edge-notched beam specimens

Hadi Haeri*

Department of Mining Engineering, Bafgh Branch, Islamic Azad University, Bafgh, Iran

(Received June 10, 2015, Revised October 19, 2015, Accepted October 22, 2015)

Abstract. A coupled experimental and numerical study of shear fracture in the edge-notched beam specimens of quasi-brittle materials (concrete-like materials) are carried out using four point bending flexural tests. The crack initiation, propagation and breaking process of beam specimens are experimentally studied by producing the double inclined edge notches with different ligament angles in beams under four point bending. The effects of ligament angles on the shear fracturing path in the bridge areas of the double edge-notched beam specimens are studied. Moreover, the influence of the inclined edge notches on the shear-fracture behavior of double edge-notched beam specimens which represents a practical crack orientation is investigated. The same specimens are numerically simulated by an indirect boundary element method known as displacement discontinuity method. These numerical results are compared with the performed experimental results proving the accuracy and validity of the proposed study.

Keywords: inclined edge notches; concrete like specimens; crack propagation; indirect shear loading; shear-fracture behavior

1. Introduction

Concrete is one of the most widely used construction material. It has a good compressive strength, a high durability and fire resistance properties. It can be casted into any structural shape which is suitable for engineering purposes. The presence of different kinds of defects called internal cracks that may be produced in a concrete specimen in its first hours of casting and even before bearing any loading conditions may extremely reduce the strength of concrete structure. The tensile and shear fracturing behaviors of concrete under different loading conditions can be estimated from the propagation of these defects (and internal cracks). A crack may act as a nucleus for the initiation and extension of new cracks in a concrete specimen in which they may in turn propagate and coalesce with each other resulting in further reduction the strength and the stiffness of the concrete. However, the mechanical characteristics of a concrete specimen may be affected by the mechanical behaviors of the defects and cracks/flaws under various loading conditions.

In the crack propagation process of brittle materials such as concrete-like specimens (double edge-cracked Brazilian disc and double edge-notched beam specimens are specially prepared from a proper mixture of Pozzolana Portland Cement (PPC), sand and water), the tensile cracks (wing

*Corresponding author, Assistant Professor, E-mail: Haerihadi@gmail.com

http://www.techno-press.org/?journal=cac&subpage=8 ISSN: 1598-8198 (Print), 1598-818X (Online)

cracks) commonly produced in indirect shear tests (disc Brazilian and four point flexure bending tests) which are observed originating from the original tips of pre-existing cracks. Brazilian disc, three and four-point bend end-notched flexure tests may be regarded as the most important tests for investigating the mixed mode (Mode I and Mode II) fracturing and determining the static and dynamic fracture toughness of concrete and rock materials. The fracturing processes and cracks propagation of various brittle materials under shear stresses may also be studied by these tests (Dai *et al*. 2011, Ayatollahi and Sistaninia 2011, Wang *et al*. 2011, Wang *et al*. 2012, Yoshihara 2013, Lancaster *et al*. 2013, Jiang *et al*. 2014, Noel and Soudki 2014, Haeri et.al. 2014a, b, Haeri 2015, Haeri et. 2015a, b). Kaplan (1961) investigated notched beams of concrete using linear elastic fracture mechanics (LEFM) under three and four point bending. Based on non-linear fracture mechanics theory, different models for predicting the fracture behavior of concretes such as the Fictitious Crack Model (FC-model) (Hillerborg 1980), the Crack Band model (Bazant and Oh 1983, Chuang and Mai 1998) and the Two Parameter Model (Jenq and Shah 1985) are investigated.

Ozcebe *et al*. (2011) a methodological approach applied to study the breakage of T-type beams and Ruiz and Carmona (2006a) studied the effect of the shape of the crack propagation on rectangular and T-type beams. On the other hand, Ruiz *et al*. (2006b) theoretically analyzed the crack initiation and propagation in the head of the beam. Savilahti *et al*. (1990) carried out direct shear tests on specimens of jointed plaster material containing non-overlapped and overlapped joints. Ghazvinian *et al*. (2011) and Sarfarazi *et al*. (2013) used particle flow code (PFC2D) to study the effect of non-overlapped and overlapped joints on the final breakage behavior of a rock bridge under direct shear tests. They compared the numerical simulations and experiment tests and confirmed that the simulated breakage paths are similar to those obtained in experiments. Zeng *et al*. (2014) predicted the fracture processes of asphalt mixture beam specimens under three-point bending by using a damage model. They analyzed the effects of crack location and coarse aggregate distribution on damage evolution behavior and crack propagation path. It has also been shown that these simulation results are in good agreement with their corresponding experimental results. Wang *et al*. (2015) studied the shear deformation in reinforced concrete beam (BRC) specimens considering low span-effective depth ratios. A multi-angle truss model was proposed to predict the diagonal crack angles. The influence of the bending moment variation along the span on the diagonal crack angles is also considered in analysis and finally experimental results. The experimental results were compared with numerical predictions of diagonal crack angles.

Many experimental works have also been devoted to study the crack initiation, propagation, interaction and eventual coalescence of the pre-existing cracks in specimens made of various substances, including natural rocks or concrete-like materials under compressive loading (Yang *et al.* 2009, Janeiro and Einstein 2010, Yang 2011, Cheng-zhi and Ping 2012).

Finite Element Method (FEM), Boundary Element Method (BEM) and Discrete Element Method (DEM) have been used for the simulation of crack propagation in brittle solids such as concrete and rock (Aliabadi and Rooke 1991, Tang 2001).

In this study, the crack propagation mechanism of pre-cracked rock like specimens is investigated experimentally by carrying out some indirect shear tests on the specially prepared samples (using a proper mixture of PPC, fine sands and water) in a concrete laboratory. The same specimens are numerically simulated by a modified higher order displacement discontinuity (HODDM) code.

The numerical simulation is developed from the higher order displacement discontinuity (e.g., Haeri 2014a, b). The special crack tip elements are used to increase the accuracy of the stress intensity factors near the crack ends. Some modifications are made in calculating the Mode I and Mode II stress intensity factors (SIFs) which result in improving the accuracy of proposed algorithm. The Maximum Tangential Stress (MTS) criterion is used to estimate the crack propagation direction based on the Linear Elastic Fracture Mechanics (LEFM) principles. The experimental results of crack propagation process are in good agreement with the numerical simulation results.

The proposed numerical method can be used in a vast variety of geomechanical projects in various engineering and bioengineering fields dealing with fracturing of solids and porous materials in continuum and discontinuous mechanics.

The experimental work is specially designed and performed to study the shear fracture in the pre-notched brittle materials. There are many novelties in the design of specimens and producing the required cracks within them.

It should be noted that in most of the published investigations, the effects of crack inclination angle and crack length on the fracturing processes of the pre-cracked concrete-like brittle materials under uniaxial compression and Brazilian disc tests have been reported. However, in current work, four points bending flexural tests are being accomplished to evaluate the shear-fracture behavior based on Mode I and Mode II stress intensity factors (SIFs) in the double inclined-edge-notched specimens of quasi-brittle materials (the notched beam concrete-like specimens specially prepared from Portland Pozzolana Cement (PPC), fine sands and water in the laboratory).

2. Fracture mechanics approach

The fracture mechanics of solids such as concretes and rocks under various loading conditions can be important in various fields of engineering and science. In fracture mechanics, due to the ability of materials to undergo plastic deformation before the failure, two types of fracturing phenomena may occur i.e. brittle and ductile. In fractures of ductile materials, extensive plastic deformation is occurred in the front of the crack so that the propagation of crack may become stable unless applied stress is increased. Mostly the Elastic-Plastic Fracture Mechanics (EPFM) concepts are used to study the fracturing behavior of plastic and elastoplastic materials (e.g., Broek 1989). In the fractures of brittle materials, relatively little plastic deformation is occurred in the front of the crack. Therefore, the propagation of crack may become instable so that it propagates rapidly without increasing in applied stress. The Linear Elastic Fracture Mechanics (LEFM) principles are quite suited for the brittle materials and still are being used by the researchers in the world (e.g., Sanford 2003). In the present study, due to the brittle behavior of concrete–like materials and rocks, LEFM concepts are being considered.

As shown in Fig. 1, LEFM suggests three types of loading modes to study the crack propagation in the pre-cracked solid materials i.e., i) Mode I (tension or opening Mode) ii) Mode II (sliding or in-plane shearing Mode) and Mode III (tearing or out of plane shearing Mode) .

Any combination of the three fracture modes, i.e., Modes I-II or II-I, I-III or III-I, II-III or III-II, I-II_III) may occur in the crack faces so-called mixed mode.

Based on the three types of loading modes, a crack propagates due to one of these three modes or by any combination of them (mixed mode). In ductile materials, the mixed mode I/III of crack propagation may be a common fracture mode (Gao and Shih 1998; Erdogan 2000), but in brittle materials (such as rock and concrete materials), the mixed mode I/II of crack propagation is more common (Whittaker *et al*.1992).

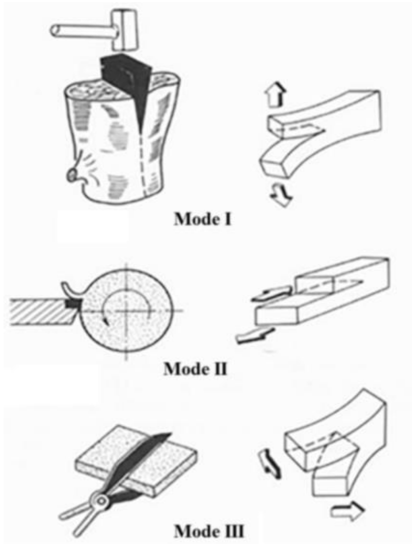

Fig. 1 Three basic modes of crack propagation (Whittaker *et al*. 1992)

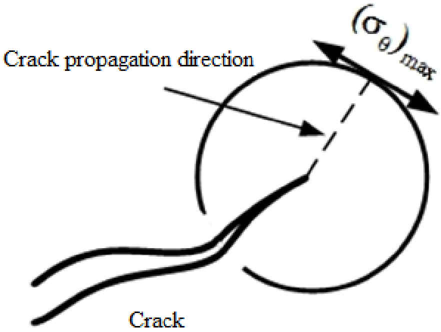

Fig.2 Crack propagation direction based on maximum tangential stress criterion (σ-criterion)

Based on the LEFM principles, three classic fracture initiation criteria were proposed to study the fracture propagation of brittle solids under mixed mode loading i.e., i) the maximum tangential stress (σ-criterion) (Erdogan and Sih 1963) ii) the maximum energy release rate (G-criterion) (Hussian and Pu 1974) and iii) the minimum strain energy density criterion (S-criterion) (Sih 1974). However, some modified form of these mentioned criteria may also be used e.g., F-criterion which is a modified form of G-criterion as proposed by Shen and Stephanson (1994) can be used to study the crack propagation of brittle materials (Haeri 2015).

σ-criterion postulates that crack growth takes place in a direction perpendicular to the maximum principal stress. Hence, this criterion requires that the maximum principal stress may be a tension stress for opening the crack along its plane as shown in Fig. 2. The prerequisites for this criterion are

$$\left.\frac{\partial \sigma_\theta}{\partial \theta}\right|_{\theta=\theta_0} = 0, \quad and \quad \frac{\partial^2 \sigma_\theta}{\partial \theta^2} < 0 \quad for \quad \sigma_\theta > 0 \tag{1}$$

Table 1 Ingredient ratios (%) and mechanical properties of the concrete specimens

Ingredients ratio (%)			Mechanical properties				
PP.cement	Fine sands	Water	Tensile strength (MPa)	Uniaxial compression strength (MPa)	Fracture toughness (MPa m1/2)	modulus of elasticity (GPa)	Poisson's ratio
44.5	22.5	33	3.81	28	0.3	17	0.21

3. Experimental studies

Some of the different types of notched beam specimens (specially prepared from concrete-like materials) are being tested in the laboratory to study the crack propagation process of the double edge notches and cracks in notched beam specimens.

3.1 Pre-cracked specimen preparation and its mechanical properties

The three-point bending notched beam specimens of quasi-brittle materials (like concrete) with 50×10×10 cm (50 cm, length, 10cm, width and 10cm, thickness) are specially prepared from a mixture of Portland Pozzolana cement (PPC), fine sands and water. Table 1 gives the ingredient ratios (%) and mechanical properties of the prepared concrete specimens tested in the laboratory before inserting the cracks.

Three-point bending test is a classical experimental procedure for measuring the Young's modulus and flexural strength of a beam in solid mechanics. This experiment is modified to be used in the study of the concrete breaking process under shear loading conditions in beam specimens containing notches and cracks.

The three-point bending notched beam specimens prepared by mixing of PPC, fine sand and water and then poured them into a steel mold with internal dimension of 50×10×10 cm. The mold contained four steel sheets bolted together plus two fiberglass plates which placed at the top and bottom of the mold (Fig. 3). The top plate had two orifices to fill the mold with the liquid mixture. The upper and the lower surfaces had slits with 1 mm. thickness and lengths equal to the width of the mold. Through these slits, notches or cracks were created by inserting two thin metallic shims with 2 mm thickness in the mold (before casting the specimens) as shown in Fig. 3.The greases added on the shims facilitated the removal of the shims. After about 7 hours; the steel shims were removed from the molds, then the specimen was prepared for testing after 28 days.

The mixture placed and hardened within the mold, each shim left an open crack in the specimen through the thickness and perpendicular to the front and back of the specimen. It seems that withdrawal of the shims does not cause any damage to the cracks.

The three-point bending tests on notched beam specimens have been used in the determination of the shear strength of concrete (Barr 1987). These tests are very sensible to eccentricity in the application of the compressive load, which is translated in flexure failure rather than shear failure. In other to solve this experimental problem, other testing methods have been proposed. For example, beams or panels under bending stresses with one or two eccentric notches and central load; or eccentric beams with two central notches and loads (Barr 1987, Shah *et al*. 1995). These test configurations allow the propagation of cracks in a mixed-mode according to fracture mechanics theories. That is, crack propagation by tension (opening) and shear (sliding of the faces) simultaneously may take place in the specimens (Shah *et al* 1995).

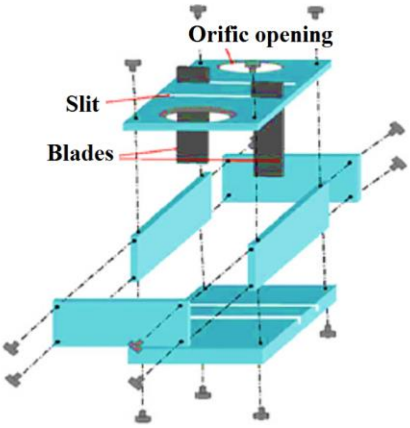

Fig. 3 Typical molds for the edge-notched beam

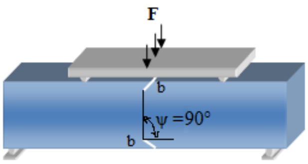

(a) ψ=90°, b=20 mm

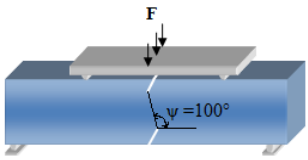

(b) ψ=100°, b=20 mm

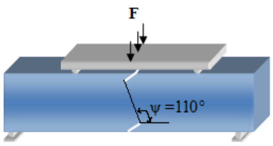

(c) ψ=110°, b=20 mm
overlapped notches

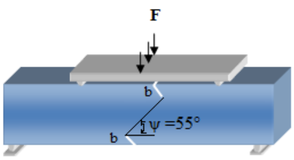

(d) ψ=55°, b=20 mm

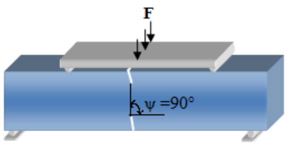

(e) ψ=90°, b=20 mm

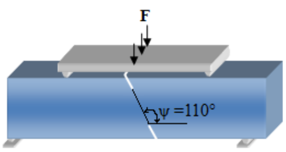

(f) ψ=110°, b=20 mm
non-overlapped notches

Fig. 4 Crack geometries showing different ligament angles, ψ, for beam specimens containing double inclined edge notches with different ligament angles and the equal notch lengths b=20 mm

In the laboratory, various types of the specially prepared double edge-notched beam (DENB) specimens are being tested to study the crack propagation process of the pre-cracked brittle solids.

The edge-notched beam specimens containing two edge cracks of different ligament angles, ψ

and crack lengths, *b* are prepared and tested in a concrete laboratory. The compressive line loading, *F* was applied and the loading rate was kept at 0.5 MPa/s during the tests.

Two edge notches with different inclination angles for double edge-notched beam specimens are shown in Fig. 4.

six modes of inclined edge notches with different ligament angles: a) overlapped notches with ligament angle, ψ=90° (Fig. 4(a)), b) overlapped notches with ligament angles, ψ=100° (Fig. 4(b)), c) overlapped notches with ligament angle, ψ=110° (Fig. 4(c)), d) non-overlapped notches with ligament angle, ψ=55° (Fig. 4(d)), e) non-overlapped notches with ligament angles, ψ=90° (Fig. 4(e)) and, f) non-overlapped notches with ligament angles, ψ=110° (Fig. 4(f)).

3.2 Effect of the inclined edge notches on the shear behavior of beam specimens

Some experiments have been carried out under bending stresses to study the effects of edge notches with inclined angles on the shear-fracture behavior of double edge-notched beam specimens.

Figs. 5 (a)-(f) illustrate the fracturing paths of overlapped (for the angles, ψ=90°, 100°, 110°) and non-overlapped edge notches (for angles, ψ=55°, 90°, 110°)

For the cases of overlapped notches shown in Figs. 5 (a) and (b) (ψ=90° and 100°), the wing cracks initiated at the crack tip and the cracks coalesced with each other at the propagating crack tips. In these failure modes, the bridge areas may fail with a single breakage surface.

For the case of overlapped notches shown in Fig. 5 (c) (for ψ=110°), the wing cracks initiated at the tip of the two original cracks and propagate in a curved path. These wing cracks developed in the intact portion and then the specimen may fail with two breakage surfaces.

For the case of non-overlapped notches shown in Figs. 5 (d) (i.e., for ψ=55°), the wing cracks initiated at the tip of the two original cracks and propagate in a curved path. In this failure mode, the specimen may fail with two breakage surfaces.

For the cases of non-overlapped notches shown in Figs. 5 (e) and (f) (ψ=90° and 110°), the wing cracks initiated at the crack tip and the cracks coalesced with each other at the propagating crack tips. In these failure modes, the bridge areas may fail with a single breakage surface.

4. Numerical simulation of the experimental tests

The displacement discontinuity method (DDM) which is a version of indirect boundary element method (IBEM) is modified by implementing a higher order displacement discontinuities variation along each boundary elements in a two dimensional elastostatic body. Several researchers used this method for stress and displacement analyses in solid mechanics (Crouch 1967a, Crouch and Starfield 1983, Tavara *et al*. 2011, Ameen *et al*. 2011, Leonel *et al.* 2012, Lei *et al*. 2012, Oliveira and Leonel2014). In this research the higher order displacement discontinuity method using special crack tip elements is employed to numerically model experimentally tested specimens.

However, it has been shown that the higher order displacement discontinuity method (HODDM) gives an accurate solution of normal displacement discontinuity (crack opening displacement) and shear displacement discontinuity (crack sliding displacement) near the crack ends. The Mode I and Mode II stress intensity factors (SIFs) can be formulated based on these discontinuities using the Linear Elastic Fracture Mechanics (LEFM) principles (Broek 1989, Sanford 2003, Crouch and Starfield 1983). This method gives very accurate results when the

(a) ψ=90°, b=20 mm

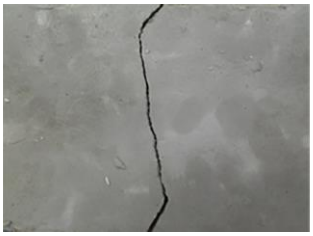

(b) ψ=100°, b=20 mm

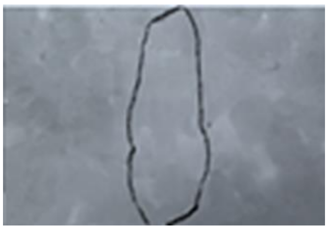

(c) ψ=110°, b=20 mm

overlapped notches

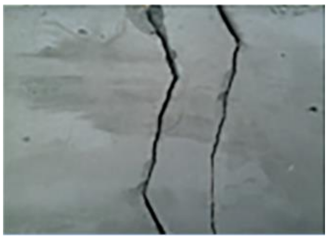

(d) ψ=55°, b=20 mm

(e) ψ=90°, b=20 mm

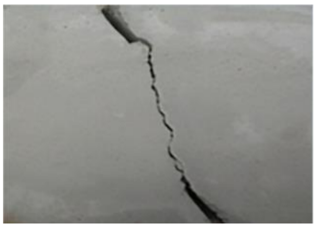

(f) ψ=110°, b=20 mm

non-overlapped notches

Fig. 5 Cracking patterns in beam specimens containing double inclined edge notches with different ligament angles and the equal notch lengths b=20 mm (a) ψ=90°; (b) ψ=100°; (c) ψ=110°; (d) ψ=55°; (e) ψ=90°; (f) ψ=110°

special crack tip elements can be used to account for the singularities of stress and displacement fields near the crack ends (Haeri 2015). This method also reduces the boundary meshes (elements) as the two sides of the line cracks are simultaneously discretized with similar boundary conditions (Haeri 2015).

4.1 Higher Order Displacement Discontinuity Method (HODDM)

The displacement discontinuities along the boundary of the problem can be achieved more

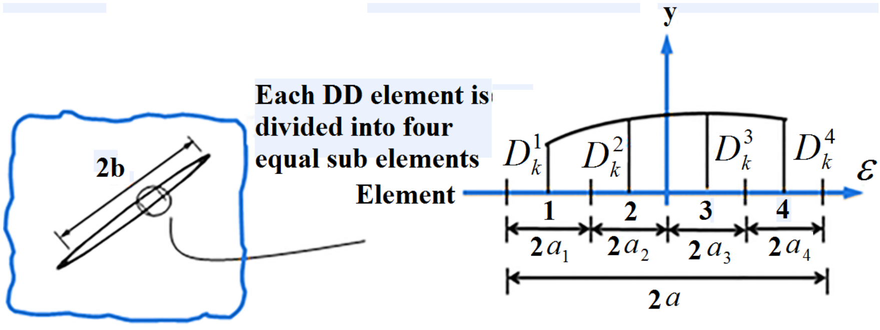

Fig. 6 Cubic collocations for the higher order displacement Discontinuity variation

accurately by using higher order displacement discontinuity (DD) elements (e.g., quadratic or cubic DD elements) in the solution of cracked elastostatic bodies.

A cubic DD element ($D_k(\varepsilon)$) is divided into four equal sub-elements that each sub-element contains a central node for which the nodal DD is evaluated numerically (the opening displacement discontinuity D_y and sliding displacement discontinuity D_x) (Haeri 2015).

$$D_k(\varepsilon) = \sum_{i=1}^{4} \Pi_i(\varepsilon) D_k^i, \quad k = x,y \tag{2}$$

Where $D_k^1(i.e. D_x^1 and\ D_y^1)$, $D_k^2(i.e. D_x^2 and\ D_y^2)$, $D_k^3(i.e. D_x^3 and\ D_y^3)$ and $D_k^4(i.e. D_x^4 and\ D_y^4)$ are the cubic nodal displacement discontinuities and

$$\begin{aligned}
\Pi_1(\varepsilon) &= -\left(3a_1^3 - a_1^2\varepsilon - 3a_1\varepsilon^2 + \varepsilon^3\right)/\left(48a_1^3\right), \\
\Pi_2(\varepsilon) &= \left(9a_1^3 - 9a_1^2\varepsilon - a_1\varepsilon^2 - \varepsilon^3\right)/\left(16a_1^3\right), \\
\Pi_3(\varepsilon) &= \left(9a_1^3 + 9a_1^2\varepsilon - a_1\varepsilon^2 - \varepsilon^3\right)/\left(16a_1^3\right), \\
\Pi_4(\varepsilon) &= -\left(3a_1^3 + a_1^2\varepsilon - 3a_1\varepsilon^2 - \varepsilon^3\right)/\left(48a_1^3\right)
\end{aligned} \tag{3}$$

are the cubic collocation shape functions using $a_1=a_2=a_3=a_4$. A cubic element has 4 nodes, which are the centers of its four sub-elements as shown in Fig. 6.

In Fig. 6, A cubic displacement discontinuity (DD) element is divided into four equal sub-elements (each sub-element contains a central node for which the nodal displacement discontinuities are evaluated numerically) (Haeri 2015).

The potential functions $f(x,y)$, and $g(x,y)$ for the cubic case can be find from

$$\begin{aligned}
f(x,y) &= \frac{-1}{4\pi(1-\nu)} \sum_{i=1}^{4} D_x^i F_i(I_0, I_1, I_2) \\
g(x,y) &= \frac{-1}{4\pi(1-\nu)} \sum_{i=1}^{4} D_y^i F_i(I_0, I_1, I_2)
\end{aligned} \tag{4}$$

in which the common function F_i, is defined as

$$F_i(I_0, I_1, I_2, I_3) = \int N_i(\varepsilon) \ln\left[(x-\varepsilon) + y^2\right]^{\frac{1}{2}} d\varepsilon, \quad \mathrm{i} = 1, \text{ to } 4 \tag{5}$$

where the integrals I_0, I_1 , I_2 and I_3 are expressed as follows

$$I_0(x,y)=\int \ln\left[(x-\varepsilon)^2+y^2\right]^{\frac{1}{2}} d\varepsilon,$$

$$I_1(x,y)=\int_{-a}^{a} \varepsilon \ln\left[(x-\varepsilon)^2+y^2\right]^{\frac{1}{2}} d\varepsilon,$$

$$I_2(x,y)=\int_{-a}^{a} \varepsilon^2 \ln\left[(x-\varepsilon)^2+y^2\right]^{\frac{1}{2}} d\varepsilon, \tag{6}$$

$$I_3(x,y)=\int_{-a}^{a} \varepsilon^3 \ln\left[(x-\varepsilon)^2+y^2\right]^{\frac{1}{2}} d\varepsilon$$

Since the singularities of the stresses and displacements near the crack ends may reduce their accuracies, special crack tip elements are used to increase the accuracy of the DDs near the crack tips (Haeri *et al* 2014 a, b, Haeri 2015). As shown in Fig. 7, the DD variation for three nodes can be formulated using a special crack tip element containing three nodes (or having three special crack tip sub-elements).

$$D_k(\varepsilon)=[\Gamma_{C1}(\varepsilon)]D_k^1(a)+[\Gamma_{C2}(\varepsilon)]D_k^2(a)+[\Gamma_{C3}(\varepsilon)]D_k^3(a), \quad k=x,y \tag{7}$$

where, the crack tip element has a length $a_1=a_2=a_3$.

Considering a crack tip element with the three equal sub-elements ($a_1=a_2=a_3$), the shape functions $\Gamma_{C1}(\varepsilon)$, $\Gamma_{C2}(\varepsilon)$ and $\Gamma_{C3}(\varepsilon)$ can be obtained as equations

$$\Gamma_{C1}(\varepsilon)=\frac{15\varepsilon^{\frac{1}{2}}}{8a_1^{\frac{1}{2}}}-\frac{\varepsilon^{\frac{3}{2}}}{a_1^{\frac{3}{2}}}+\frac{\varepsilon^{\frac{5}{2}}}{8a_1^{\frac{5}{2}}},$$

$$\Gamma_{C2}(\varepsilon)=\frac{-5\varepsilon^{\frac{1}{2}}}{8a_1^{\frac{1}{2}}}+\frac{3\varepsilon^{\frac{3}{2}}}{2\sqrt{3}a_1^{\frac{3}{2}}}-\frac{\varepsilon^{\frac{5}{2}}}{4\sqrt{3}a_1^{\frac{5}{2}}}, \tag{8}$$

$$\Gamma_{C3}(\varepsilon)=\frac{3\varepsilon^{\frac{1}{2}}}{8\sqrt{5}a_1^{\frac{1}{2}}}-\frac{\varepsilon^{\frac{3}{2}}}{2\sqrt{5}a_1^{\frac{3}{2}}}+\frac{\delta^{\frac{5}{2}}}{8\sqrt{5}a_1^{\frac{5}{2}}}$$

$$F_C(x,y)=\frac{-1}{4\pi(1-\nu)}\int_{-a}^{a} D_k(\varepsilon)\ln\left[(x-\varepsilon)^2+y^2\right]^{\frac{1}{2}} d\varepsilon,\ k=x,y \tag{9}$$

Inserting the common displacement discontinuity function, $D_k(\varepsilon)$ (Eq. (7)) in Eq. (9) gives

$$F_C(x,y)=\frac{-1}{4\pi(1-\nu)}\{[\int_{-a}^{a}\Gamma_{C1}(\varepsilon)\ln\left[(x-\varepsilon)^2+y^2\right]^{\frac{1}{2}} d\varepsilon]D_k^1+ \\ [\int_{-a}^{a}\Gamma_{C2}(\varepsilon)\ln\left[(x-\varepsilon)^2+y^2\right]^{\frac{1}{2}} d\varepsilon]D_k^2+[\int_{-a}^{a}\Gamma_{C3}(\varepsilon)\ln\left[(x-\varepsilon)^2+y^2\right]^{\frac{1}{2}} d\varepsilon]D_k^3,\ k=x,y \tag{10}$$

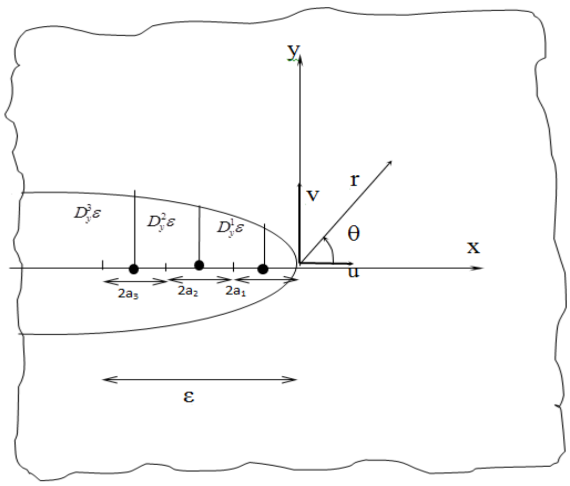

Fig. 7 A special crack tip element with three equal sub-elements

Inserting the shape functions $\Gamma_{C1}(\delta)\varepsilon$, $\Gamma_{C2}(\delta)\varepsilon$ and $\Gamma_{C3}(\delta)\varepsilon$ in Eq. (10) after some manipulations and rearrangements the following three special integrals are deduced

$$
\begin{aligned}
I_{C1}(x,y) &= \int_{-a}^{a} \varepsilon^{\frac{1}{2}} \ln\left[(x-\varepsilon)^2 + y^2\right]^{\frac{1}{2}} d\varepsilon, \\
I_{C2}(x,y) &= \int_{-a}^{a} \varepsilon^{\frac{3}{2}} \ln\left[(x-\varepsilon)^2 + y^2\right]^{\frac{1}{2}} d\varepsilon \\
I_{C3}(x,y) &= \int_{-a}^{a} \varepsilon^{\frac{5}{2}} \ln\left[(x-\varepsilon)^2 + y^2\right]^{\frac{1}{2}} d\varepsilon
\end{aligned}
\tag{11}
$$

Based on the linear elastic fracture mechanics (LEFM) principles, the Mode I and Mode II stress intensity factors KI and KII, (expressed in MPa $m^{1/2}$) can be written in terms of the normal and shear displacement discontinuities obtained for the last special crack tip element as (Shou 2000a)

$$
K_I = \frac{\mu}{4(1-\nu)}\left(\frac{2\pi}{a_1}\right)^{\frac{1}{2}} D_y(a_1), \quad \text{and} \quad K_{II} = \frac{\mu}{4(1-\nu)}\left(\frac{2\pi}{a_1}\right)^{\frac{1}{2}} D_x(a_1) \tag{12}
$$

where μ is the shear modulus and v is Poisson's ratio of the brittle material.

4.2 Cracking boundaries for double edge-notched beam specimens

In the simulation of the double edge-notched beam specimens, the discretization of the cracking boundaries have been accomplished by using 38 cubic elements along beam specimens, 8 cubic elements along each pre-existing crack (Fig. 8). In the numerical modeling, the ratio of crack tip length, L to the crack length, b is 0.2 (L/b =0.2) and three special crack tip elements are used.

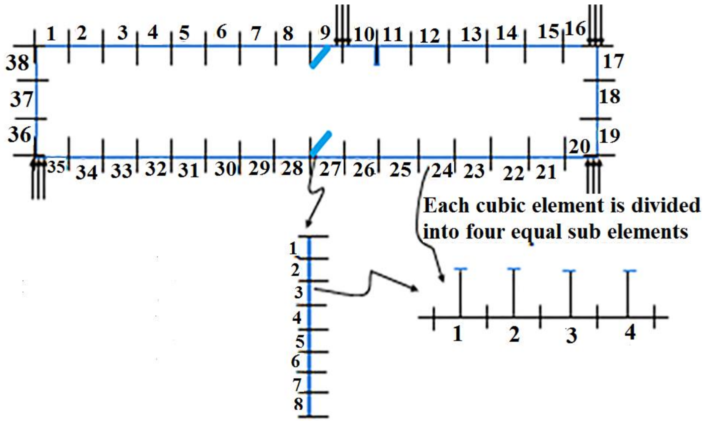

Fig. 8 discretization of the cracking boundaries for double edge-notched beam specimen

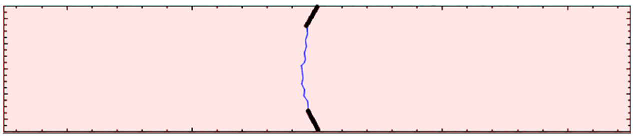

(a) ψ=90°, *b*=20 mm

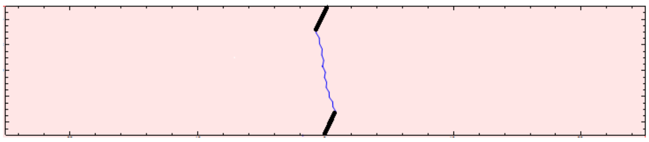

(b) ψ=100°, *b*=20 mm

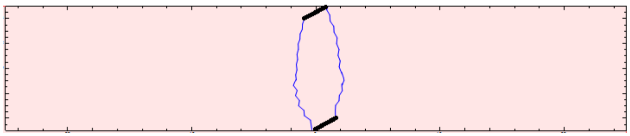

(c) ψ=110°, *b*=20 mm

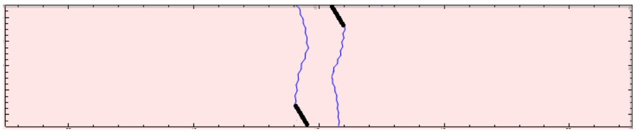

(d) ψ=45°, *b*=20 mm

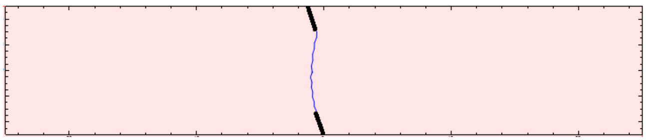

(e) ψ=45°, *b*=20 mm

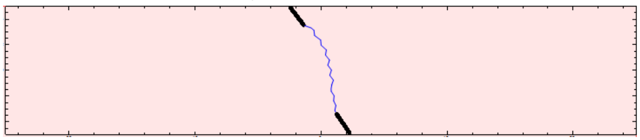

(f) ψ=45°, *b*=20 mm

Fig. 9 Numerical simulation of crack propagation paths and cracks coalescence for the double edge-notched beam (DENB) inclined notches under four-point bending

Table 2 Comparing the wing crack initiation and breakage loads (using the proposed code and experiments)

Crack geometries	Experimental			Numerical		
	Wing crack initiation load (N)		Beam breakage load	Wing crack initiation load (N)		Beam breakage load
	Upper crack	Lower crack		Upper Crack	Lower crack	
(a) ψ =90°, b=20 mm	620	590	940	640	580	950
(b) ψ =100°, b=20 mm	780	710	1250	800	720	1240
(c) ψ =110°, b=20 mm	550	520	1140	530	530	1150
(d) ψ =55°, b=20 mm	890	840	1410	870	840	1430
(e) ψ =90°, b=20 mm	940	910	1620	930	930	1610
(f) ψ =110°, b=20 mm	920	870	1570	930	860	1580

4.3 Numerical simulation of the experimental works

Although the experiments carried out in this study are in three dimensions the numerical simulation of them is done by a two-dimensional higher order displacement discontinuity briefly explained in the previous section. This numerical analysis is based on the two dimensional plain strain conditions which are more usual in fracture mechanics literature. The numerical crack paths has been calculated in different steps by incrementally extending crack length in the direction of θ for about 1-2 mm in each step. However, in the present research, the crack propagation path has been estimated by the iterative method and the coalescence of the cracks in specimens containing pre-existing cracks/flaws or holes has been observed. In this iterative method, the cubic displacement discontinuity elements (using higher order elements) give accurate results for the Mode I and Mode II stress intensity factors.

The double edge-notched beam specimens with inclined notches as shown in Figs. 5 (a)-(f) are numerically simulated by the modified (HODDM) code. The corresponding numerical results are illustrated in Figs. 9 (a)-(f).

In the present numerical simulations, the Mode I and Mode II stress intensity factors (SIFs) proposed by Irwin (2000a) are estimated based on LEFM approach. A boundary element code is provided using the maximum tangential stress criterion given by Erdogan and Sih (1963) in a stepwise procedure so that the propagation paths of the propagating wing cracks are estimated. As shown in Figs. 9(a)-(f), the simulated propagation paths are in good agreement with the corresponding experimental results already explained in this paper.

Table 2 compares the numerical and experimental results considering the crack initiation and breakage loads of concrete like specimens under four points bending flexural test. These comparisons give a better knowledge of the crack propagation mechanism and breakage of concrete -like specimens. The failure loads for various samples changes from 940-1620 N for the experimental works and from 950-1610 N for the numerical approach.

5. Discussions

Let consider a rectangular specimen containing inclined edge notch with height, $2h$, width, W, the normal stress, σ=1 MPa and the Poisson's ratio, v=0.1 as shown in Fig. 8. The analytical

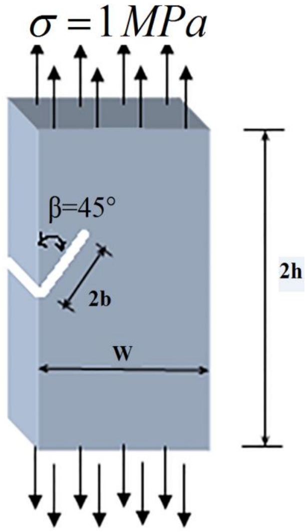

Fig. 10 a rectangular specimen containing inclined edge notch with *W/h*=1, *b/W*=0.3, *W*=50 mm

solution of this typical fracture mechanics problem is given by Bowie (1973) as. Based on Fig.10, the analytical solution for Mode I and Mode II stress intensity factors (SIFs) in an inclined edge-notched specimen can be estimated from

$$K_I = 0.884\sigma\sqrt{\pi b} \text{ and } K_{II} = 0.451\sigma\sqrt{\pi b} \tag{13}$$

The normalized Mode I and Mode II SIFs are simplified as

$$\begin{aligned} K_I^N &= \frac{K_I}{\sigma\sqrt{\pi b}} \\ K_{II}^N &= \frac{K_{II}}{\sigma\sqrt{\pi b}} \end{aligned} \tag{14}$$

The normalized analytical values of K_I^N and K_{II}^N can be estimated from Eq. (13) as 0.884 and 0.451, respectively.

The inclined edge crack problem (Fig. 10) has numerically solved by the proposed approach and the results are compared with the analytical results.

Table 3 shows the effect of the number of elements which show the accuracy of the proposed method. The table illustrates the high accuracy of the proposed boundary element method by using a relatively small number of elements (about 8 cubic displacement discontinuity elements containing thirty two nodes).

The crack propagation process in brittle materials has been studied by several researches using the edge cracked problem under shear loading.

Liu (2003) has been numerically (using a 2-D finite element code) investigated the crack propagation patterns of the single-cracked disc and edge notched beam specimens. He has used the R-T2D code (R-T2D code based on FEM coupled with the Rock Fracture process analysis (RFPA) model) to conduct a number of numerical simulations.

Table 3 The analytical and numerical values of the Mode I and Mode II stress intensity factors K_I^N, and K_{II}^N for the rectangular specimen containing inclined edge notch using different number of elements along the crack (L/b=0.1)

Number of elements	K_I^N		K_{II}^N	
	HODDM	Analytic	HODDM	Analytic
2	0.896	0.884	0.457	0.451
4	0.891	0.884	0.455	0.451
6	0.888	0.884	0.453	0.451
8	0.885	0.884	0.451	0.451
10	0.884	0.884	0.451	0.451

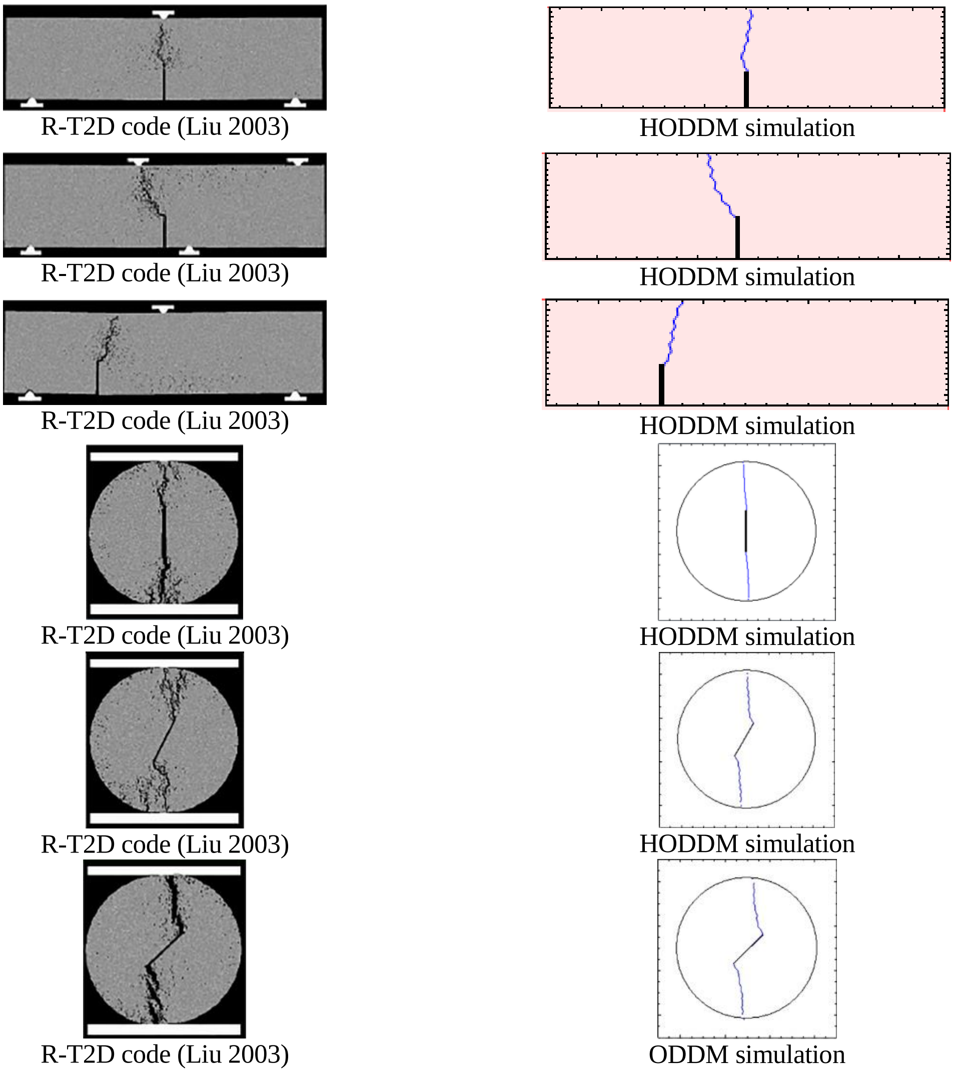

Fig. 11 Crack propagation paths in the single-cracked disc and edge notched beam specimens from the R-T^{2D} code (Liu 2003) and HODDM simulation

Figs. 11 show the crack propagation of the single-cracked disc and edge notched beam specimens in the R-T2D and HODDM simulations, respectively.

The crack initiation and propagation in single cracked disc and edge notched beam specimens in HODDM2D model are in good agreement with the numerical results (using the R-T^{2D} code) given by Liu (2003). High accuracy of the proposed numerical results (obtained by using HODDM) is illustrated in Fig. 9 by comparing these results with those given by using finite element method (using the R-T^{2D} code). It should be noted that the number of elements used in HODDM is much lower than those used in FEM. These comparisons give a better knowledge of the crack propagation mechanism and breaking of the brittle materials such as concrete and rock specimens.

6. Conclusions

The mechanism of crack propagation in brittle solids under shear stress has been experimentally and numerically investigated. Such a complicated process needs a further research to investigate the crack propagation, cracks coalescence and final breakage paths (for example for a rock bridge area under four point bending specimens).

To investigate the fracturing process in brittle solids under shear loading conditions, some shear tests were conducted on concrete beam specimens (each specimen contains two edge cracks). Therefore, various types of the specially prepared double edge-notched beam specimens are being tested to study the crack propagation process of the pre-cracked brittle solids. These specimens (with different ligament angles and the equal notch lengths) are tested in the laboratory. The Effects of the inclined edge notches on the shear-fracture behavior in beam specimens are also investigated.

A modified higher order displacement discontinuity method, (which is a category of the broad boundary element method) is especially modified to simulate the mechanism of crack propagation and cracks coalescence in the double edge-notched beam specimens.

It can be concluded that in non-overlapped notches with high ligament angles, the cracks are initiated from both two cracks tips and the elliptical breaking surface may occur in the specimens, but for lower ligament angles, the cracks may propagate to coalesce with each other at the propagating crack tips and the specimen may fail at a single fracturing surface.

In overlapped notches with lower ligament angles, the cracks are initiated from both tips of cracks and the specimen may fail at two fracturing surface. It has been shown that the shear fracturing of double edge-notched specimens occur mainly by the propagation of wing cracks emanating from the tips of the two inclined notches. Kink cracks may be produced in some of the beam specimens with inclined notches due to propagation and coalescence of the primarily induced wing cracks.

The numerical models well illustrate the shear behavior of the double edge-notched beam specimens. These models also demonstrate that the cracks propagation paths produced by the coalescence phenomenon of the non-overlapped and overlapped notches.

In this study, it has been shown that there is a good agreement between the corresponding numerical and experimental results which enables one to clearly understand the fracturing mechanism of concrete-like specimens containing edge notches or cracks.

Acknowledgements

This work is sponsored by Iran's National Elites Foundation (INEF). Partial supports of center of excellence for structures and earthquake engineering at Sharif University of technology is greatly appreciated.

References

Aliabadi, M.H. (1991), Rooke DP Numerical fracture mechanics, Computational Mechanics Publications, Southampton, U.K.

Ameen, M., Raghu Prasad, B.K. and Gopalakrishnan, A.R. (2011), "Modeling of concrete cracking-A hybrid technique of using displacement discontinuity element method and direct boundary element method", *Eng. Anal. Bound. Elem.*, **35**, 1054-1059.

Ayatollahi, M.R. and Sistaninia, M. (2011), "Mode II fracture study of rocks using Brazilian disk specimens", *Int. J. Rock Mech. Min. Sci*., **48**, 819-826.

Barr, B. (1987), "The fracture characteristics of FRC materials in shear, fiber reinforced concrete: properties and applications", SP -105, Editado por S. P. Shah y B. Batson, American Concrete Institute.

Bazant, Z.P. and Oh, B.H. (1983), "Crack band theory for fracture of concrete", *Mater. Struct*., **16**, 155-77.

Bowie, O.L. (1973), *Solution of Plane Crack Problems by Mapping Technique, In Methods of Analysis and Solution of Crack Problems*, Ed. G.C. Sih, Lehigh University, Bethlehem, Pennsylvania.

Broek, D. (1989), *The Practical Use of Fracture Mechanics*, 4th Edition, Kluwer Academic Publishers, Netherland.

Cheng-zhi, P. and Ping, C. (2012), "Breakage characteristics and its influencing factors of rock-like material with multi-fissures under uniaxial compression", *Trans. Nonferrous Met. Soc. China*, **22**, 185-191.

Chuang, T. and Mai, Y. (1998), "Flexural behavior of strain-softening solids", *Int. J. Solid. Struct.*, **25**, 1427-1443.

Crouch, S.L. (1957a), "Analysis of stresses and displacements around underground excavations: an application of the Displacement Discontinuity Method", University of Minnesota Geomechanics Report, Minneapolis, Minnesota.

Crouch, S.L. and Starfield, A. (1983), *Boundary Element Methods in Solid Mechanics*, Allen and Unwin, London.

Dai, F., Xia, K., Zheng, H. and Wang, Y.X. (2011), "Determination of dynamic rock mode-I fracture parameters using cracked chevron notched semi-circular bend specimen", *Eng. Fract. Mech*., **78**, 2633-2644.

Erdogan, F. and Sih, G.C. (1963), "On the crack extension in plates under loading and transverse shear", *J. Fluid. Eng*., **85**, 519-527.

Ghazvinian, A., Sarfarazi, V., Schubert, W. and Blumel, M. (2011), "A study of the failure mechanism of planar non-persistent open joints using PFC^{2D}", *Rock Mech. Rock Eng*., **45**, 677-693.

Haeri, H., Shahriar K., Marji, M.F. and Moarefvand, P. (2014a), "Experimental and numerical study of crack propagation and coalescence in pre-cracked rock-like disks", *Int. J. Rock Mech. Min. Sci*., **67c**, 20-28.

Haeri, H., Khaloo, A. and Marji, M.F. (2014b), "Fracture analyses of different pre-holed concrete specimens under compression", *Acta Mechanica Sinica*, DOI:10.1007/s10409-015-0436-3.

Haeri, H. (2015), *Coupled Experimental-Numerical Fracture Mechanics*, Lambert Academic Press, Germany.

Haeri, H., Shahriar, K., Marji, M.F. and Moarefvand, P. (2015a), "On the crack propagation analysis of rock like Brazilian disc specimens containing cracks under compressive line loading", *Latin Am. J. Solid. Struct.*, **11**(8), 1400-1416.

Haeri, H., Shahriar K., Marji, M.F. and Moarefvand, P. (2015b), "On the HDD analysis of micro cracks

initiation, propagation and coalescence in brittle substances", *Arab. J. Geoscie.*, **8**, 2841-2852.
Hillerborg, A. (1980), "Analysis of fracture by means of the fictitious crack model, particularly for fiber reinforced concrete", *Int. J. Cement Compos.*, **2**, 177-190.
Hussian, M.A., Pu, E.L. and Underwood, J.H. (1974) "Strain energy release rate for a crack under combined mode I and mode II. In: Fracture analysis", ASTM STP 560. American Society for Testing and Materials, 2-28.
Irwin, G.R. (1957), "Analysis of stress and strains near the end of a crack", *J. Appl. Mech*., **24**, 361.
Janeiro, R.P. and Einstein, H.H. (2010), "Experimental study of the cracking behavior of specimens containing inclusions (under uniaxial compression)", *Int. J. Fract.*, **164**, 83-102.
Jenq, Y.S. and Shah, S.P. (1985), "Two parameter fracture model for concrete", *J. Eng. Mech*., **111**, 1227-1241.
Jiang, Z., Wan, S., Zhong, Z., Li, M. and Shen, K. (2014), "Determination of mode-I fracture toughness and non-uniformity for GFRP double cantilever beam specimens with an adhesive layer", *Eng. Fract. Mech.*, **128**, 139-156.
Kaplan, M.F. (1961), "Crack propagation and the fracture of concrete", *ACI J*., **58**, 591-610.
Lancaster, I.M., Khalid, H.A. and Kougioumtzoglou, I.A. (2013), "Extended FEM modelling of crack propagation using the semi-circular bending test", *Constr. Build. Mater.*, **48**, 270-277.
Leonel, E.D., Chateauneuf, A. and Venturini, W.S. (2012), "Probabilistic crack growth analyses using a boundary element model: Applications in linear elastic fracture and fatigue problems", *Eng. Anal. Bound. Elem.*, **36**, 944-959.
Lei, J., Wang, Y.S., Huang, Y., Yang, Q. and Zhang, C. (2012), "Dynamic crack propagation in matrix involving inclusions by a time-domain BEM", *Eng. Anal. Bound. Elem.*, **36**, 651-57.
Liu, H. (2003), "Numerical modelling of the rock fracture process under mechanical loading", Thesis, LULEA university of technology, Sweden.
Noel, M. and Soudki, K. (2014), "Estimation of the crack width and deformation of FRP-reinforced concrete flexural members with and without transverse shear reinforcement", *Eng. Struct.*, **59**, 393-398.
Oliveira, H.L. and Leonel, E.D. (2014), "An alternative BEM formulation, based on dipoles of stresses and tangent operator technique, applied to cohesive crack growth modeling", *Eng. Anal. Bound. Elem.*, **41**, 74-82.
Ozcebe, G. (2011), "Minimum flexural reinforcement for T-beams made of higher strength concrete", *Can. J. Civil Eng.*, **26**, 525-534.
Ruiz, G. and Carmona, R.J. (2006a), "Experimental study on the influence of the shape of the cross-section and the rebar arrangement on the fracture of LRC beams", *Mater. Struct.*, **39**, 343-352.
Ruiz, G., Carmona J.R. and Cendón, D.A. (2006b), "Propagation of a cohesive crack through adherent reinforcement layers", *Comput. Meth. Appl. Mech. Eng.*, **195**, 7237-7248.
Sanford, R.J. (2003), *Principles of Fracture Mechanics*, Pearson Education, hIC., Upper Saddle River, New Jersey.
Sarfarazi, V., Ghazvinian, A., Schubert, W., Blumel, M. and Nejati, H.R. (2014), "Numerical Simulation of the Process of Fracture of Echelon Rock Joints", *Rock. Mech. Rock. Eng*., **47**, 1355-1371.
Savilahti, T., Nordlund, E. and Stephansson, O. (1990), "Shear box testing and modeling of joint bridge", *Proceedings of international symposium on shear box testing and modeling of joint bridge Rock Joints*, Norway.
Shah, S., Swartz, S.Y. and Ouyang, C. (1995), *Fracture Mechanics of concrete: Applications of Fracture Mechanics to Concrete, Rock, and Other Quasi-Brittle Materials*, John Wiley & Sons, New York.
Shou, K.J. (2000a), "A novel superposition scheme to obtain fundamental boundary element solutions in multi-layered elastic media", *Int. J. Numer. Anal. Meth. Geomech*., **24**(10), 795-814.
Shen, B. and Stephansson, O. (1994), "Modification of the G-criterion for crack propagation subjected to compression", *Eng. Fract. Mech*., **47**, 177-189.
Sih, G.C. (1974), "Strain-energy-density factor applied to mixed mode crack problems", *Int. J. Fract*., **10**, 305-321.
Tang, C.A., Lin, P., Wong, R.H.C. and Chau, K.T. (2001), "Analysis of crack coalescence in rock-like

materials containing three flaws- Part II: Numerical approach", *Int. J. Rock Mech. Min. Sci*., **38**, 925-939.
Tavara, L., Mantic, V., Graciani, E. and París, F. (2011), "BEM analysis of crack onset and propagation along fiber-matrix interface under transverse tension using a linear elastic-brittle interface model", *Eng. Anal. Bound. Elem.*, **35**, 207-222.
Wang, Q.Z., Feng, F., Ni, M. and Gou, X.P. (2011), "Measurement of mode I and mode II rock dynamic fracture toughness with cracked straight through flattened Brazilian disc impacted by split Hopkinson pressure bar", *Eng. Fract. Mech*., **78**, 2455-2469.
Wang, Q.Z., Gou, X.P. and Fan, H. (2012), "The minimum dimensionless stress intensity factor and its upper bound for CCNBD fracture toughness specimen analyzed with straight through crack assumption", *Eng. Fract. Mech*., **82**, 1-8.
Wang, T., Dai, J.G. and Zheng, J.J. (2015), "Multi-angle truss model for predicting the shear deformation of RC beams with low span-effective depth ratios", *Eng. Struct.*, **91**, 85-95.
Whittaker, B.N., Singh, R.N. and Sun, G. (1992), *Rock Fracture Mechanics, Principles, Design and Applications*, Elsevier, Netherlands.
Wong, R.H.C., Leung, W.L. and Wang, S.W. (2001), *Shear strength study on rock-like models containing arrayed open joints*, Eds. Elsworth, D., Tinucci, J.P., Heasley, K.A., Rock mechanics in the national interest. Swets & Zeitlinger Lisse, Leiden.
Yang, Q., Dai, Y.H., Han, L.J. and Jin, Z.Q. (2009), "Experimental study on mechanical behavior of brittle marble samples containing different flaws under uniaxial compression", *Eng. Fract. Mech*., **76**, 1833-1845S
Yang, S.Q. (2011), "Crack coalescence behavior of brittle sandstone samples containing two coplanar fissures in the process of deformation breakage", *Eng. Fract. Mech*., **78**, 3059-3081.
Yoshihara, H. (2013), "Initiation and propagation fracture toughness of solid wood under the mixed Mode I/II condition examined by mixed-mode bending test", *Eng. Fract. Mech.*, **104**, 1-15.
Zeng, G.,Yang, X., Yina, A. and Bai, F. (2014), "Simulation of damage evolution and crack propagation in three-point bending pre-cracked asphalt mixture beam", *Constr. Build. Mater.*, **55**, 323-332.

CC